ORIGINAL RESEARCH

Single-Cell RNA Sequencing Reveals the Immune Cell Profiling in IMQ Induced Psoriasis-Like Model

Shasha Jin [iD]*, Yixin Wang*, Chenxin Qie, Lu Yang, Yinhao Wu, Tingting Zhang, Jianwen Di, Jun Liu

New Drug Screening Center, Institute of Pharmaceutical Sciences, China Pharmaceutical University, Nanjing, 210009, People's Republic of China

*These authors contributed equally to this work

Correspondence: Jun Liu, New Drug Screening Center, China Pharmaceutical University, Nanjing, 210009, People's Republic of China, Tel +86-25-83271043, Fax +86-25-83271142, Email junliu@cpu.edu.cn

Purpose: Psoriasis is a chronic systemic inflammatory skin disease with a high recurrence rate. The immune response plays an important role in psoriasis. However, the subsets of immune cells involved in inflammation in psoriatic mice have not been fully studied. This study showed the immune environment characteristics of psoriasis in mice.

Methods: We used single-cell RNA sequencing (10× Genomics) as an unbiased analytical strategy to investigate the heterogeneity of skin immune cells in imiquimod-induced psoriasis mice systematically.

Results: We identified 10 major clusters and their marker genes among 14,439 cells. The proportions of macrophages, NK/T cells, conventional dendritic cells (cDCs) and plasmacytoid dendritic cells (pDCs) were increased in psoriatic mice. Macrophages were the largest group and were further divided into 7 subgroups, and all macrophage clusters were increased in psoriatic mice. Differentially expressed genes in control versus psoriatic mice skin lesions showed that Fcgr4, Saa3 and Acp5 in macrophages, Acp5, Fcgr4 and Ms4a6d in NK/T cells, Saa3 in cDCs, and Ifitm1 in pDCs were upregulated in psoriasis mice. Kyoto Encyclopedia of Genes and Genomes (KEGG) signaling pathway enrichment analysis emphasized the role of oxidative phosphorylation signals and antigen processing and presentation signals in murine psoriasis-like models.

Conclusion: Our study reveals the immune environment characteristics of the commonly used IMQ induced psoriasis-like models and provides a systematic insight into the immune response of mice with psoriasis, which is conducive to comparing the similarities and differences between the mouse model and human psoriasis.

Keywords: single-cell RNA sequencing, psoriasis, imiquimod, immune cells

Introduction

Psoriasis is a prevalent, chronic inflammatory skin disease that affects approximately 2–3% of the world's population.[1] It has the characteristics of long course and easy recurrence, which has a bad impact on the spirit and life of patients.[2] The most common clinical manifestations are erythematous, scaling lesions that affect both genders. Chronicity and distal effects of psoriasis-related inflammation lead to many complications in affected patients, including arthritis, metabolic syndrome, cardiovascular disease and respiratory involvement.[3–6]

The pathogenesis of psoriasis is complex and has not been fully elucidated, among which immune abnormalities are an important reason. A large number of studies have shown that psoriasis is an immune-mediated inflammatory skin disease, and its pathogenesis is related to inflammatory cell and inflammatory factor infiltration.[7,8] It is well known that dendritic cells (DCs) play a key role in the initiation and maintenance of psoriasis, but their activation in psoriasis is not entirely clear.[9] Some studies have found that macrophages contribute to the pathogenesis of psoriasis, especially in the initiation stage.[10] In addition, T cells and neutrophils play an important role in the occurrence and development of psoriasis.[11,12] Thus, psoriasis and immunity are inseparable and it is necessary to reveal the immune cell spectrum of psoriasis mice.

Graphical Abstract
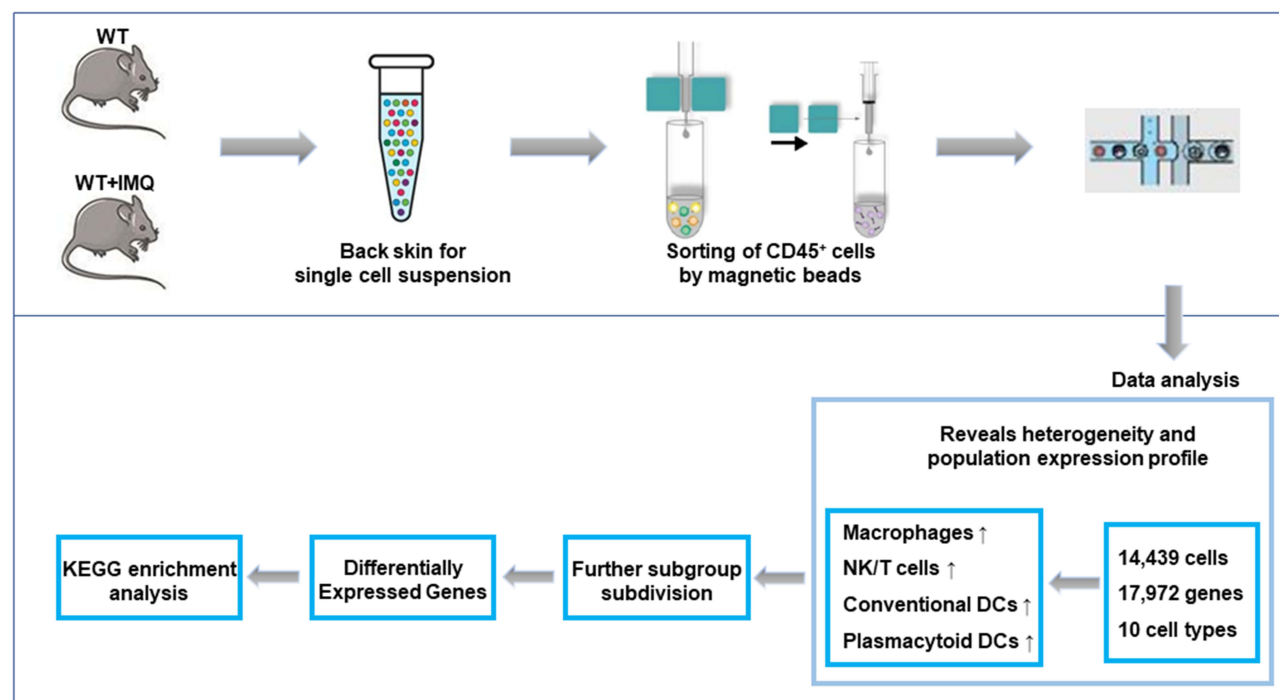
Imiquimod (IMQ) is a Toll-like receptor (*Tlr7/8*) agonist that can be applied to mouse skin to elicit erythema, scaling, keratinocyte proliferation with acanthosis, altered keratinocyte differentiation (parakeratosis), and a dermal infiltrate that includes T cells.[13] In recent years, topical application of IMQ cream to murine skin has increasingly been used as an acute psoriasiform murine model, in part due to its convenience and ability to elicit dermatitis resembling some aspects of psoriasis.[14] This study also used IMQ to construct psoriasis-like mice.

Single cell RNA sequencing (scRNA-seq) is a new technique for transcriptome sequencing at the single cell level. It has the characteristics of high throughput and high cell resolution and can realize the division of cell groups and the detection of gene expression differences between cell groups. More and more studies have used this technology to reveal the cell map of specific tissues, which has brought significant breakthroughs in the understanding of diseases. Recently, this technique has also been used to study the characteristics of human psoriasis[15–17] mainly to analyze CD45$^+$ cells, but the immune cell spectrum of IMQ-induced psoriasis mice is still unclear.

Here, we used 10× Genomics technology[18] as a powerful tool for unbiased and systematic studies to reveal the immune cell spectrum of IMQ-induced psoriasis mice. A total of 14,439 immune cells were identified. Next, we further performed single-cell trajectory analysis and pathway enrichment analysis. The transcriptional landscape and phenotypic heterogeneity of psoriatic skin immune cells were revealed unprecedently, and their gene expression signatures were identified, suggesting specialized functions. Our results promote the understanding of psoriasis immunity in mice and contribute to the development of inflammatory treatments for psoriasis.

Materials and Methods
Mice and Treatments
The wild-type C57BL/6J female mice (6~7 weeks old) were obtained from Beijing Vital River Laboratory Animal Technologies Co. Ltd, where they were reared under specific pathogen-free conditions. Before the experiment, these mice were allowed to adapt to our environment for a week. All our animal experiments were carried out according to the

Laboratory Animal Management Committee of Jiangsu Province and approved by the ethics committee of China Pharmaceutical University (Nanjing, China, 2020–12-007).

First, shave hair on the back skin and right ear of the mouse, and then 62.5 mg of commercially available IMQ cream (5%) (obtained from Imiquimod cream; Sichuan Med-Shine Pharmaceutical Co. Ltd, China) was continuously applied to these sites for 5 days. The thickness of the right ear, which was used to evaluate epidermal inflammation and proliferation, was repeatedly measured with a micrometer at the indicated days. One day after the end of IMQ application, mice were killed by exsanguination from the abdominal aorta and posterior vena cava under isoflurane inhalation anesthesia. The back skin tissue was removed from each mouse and stored for further use.

Histological Analysis

The skin samples were fixed with formaldehyde and embedded in paraffin for histopathological analysis by hematoxylin eosin (H&E) staining. Five slices per mouse for microscopic analysis to evaluate the disease status of mice. We used Olympus bx53 microscope to observe the slices. The thickness of the epidermis was quantified using the ImageJ software.

Immunohistochemistry (IHC)

Paraffin embedded sections were routinely processed. Briefly, we used xylene and ethanol to deparaffinize and rehydrate the tissues. Slides for immunostaining for F4/80 (GB11027, Servicebio) were pretreated with citrate buffer in a microwave oven. Antibody dilutions were 1:1000. Quantification was performed through counting positive cells in 6 to 10 high-powered fields (magnification, ×200) with a blinded fashion.

Tissue Dissociation and Sorting for Single-Cell RNA-Seq

Skin samples from the back lesions of 5 control or 5 psoriatic mice were mixed to prepare samples for isolation of viable cells. The back skins were finely minced and then incubated in a digestion solution containing RPMI, 0.28 mg/mL Liberase TM (Roche) and 0.2 mg/mL DNase (Sigma-Aldrich) for 1.5 hours at 37°C. During digestion, the centrifuge tubes were gently upside down and mixed every 5 minutes. The dissociated cells were filtered through a 40 μm cell filter to get single cell suspensions and then subjected to red blood cell lysis. 10 μL cell suspension was stained with trypan blue to observe cell viability.

The cell viability was more than 80% and CD45$^+$ sorting was performed. The cells were placed in a sorting buffer (pH7.2, phosphate buffer containing 0.5% BSA and 2mM EDTA) containing CD45 microbeads (Miltenyi Biotec) and sorted on the LS sorting column (Miltenyi Biotec). Cells labeled by magnetic beads were retained on the sorting column and were collected.

Droplet-Based Single-Cell RNA-Seq

Single cell suspension was loaded onto a chromium single cell controller (10× Genomics) and cells entered nanoliter-scale Gel Bead-In Emulsions (GEMs). Here, GEM contained barcode, Unique Molecular Index (UMI), primer, enzyme Gel Beads and single cells. Cell cleavage, reverse transcription, amplification completed in GEMs, in which all generated cDNAs share a common 10x barcode. 10x Barcodes were used to associate individual reads back to the individual partitions. Then, Illumina-ready sequencing libraries were produced and sequenced. Transcripts were mapped to the mm10-3.0.0 reference genome.

Immune repertoire measurement and gene expression at single cell resolution were conducted using Chromium Single Cell V(D)J Reagent Kit following the manufacturer's instructions.

Other data and analytical procedures can be obtained from the corresponding authors with reasonable request. The raw sequencing data generated from this study have been deposited in NCBI SRA under the accession number SRP 268188 (WT+IMQ) and SRP 14116707 (WT). The cDNA/DNA/small RNA libraries were sequenced on the Illumina sequencing platform by Genedenovo Biotechnology Co., Ltd. (Guangzhou, China).

Single-Cell RNA-Seq Quality Control

We filtered cells according to a series of standards to retain high-quality cells. Cell Ranger analysis software was used to filter and compare the raw data. Seurat was used for further cell filtration. We kept cells with genes between 500 and 4000. Cells with more than 10,000 UMIs and more than 10% mitochondrial gene expression were excluded. Finally, 14,439 qualified cells were left for downstream analysis.

Single-Cell RNA-Seq Data Processing

The data were homogenized after removing low-quality cells. To eliminate batch effects, Seurat anchors cells via canonical correspondence analysis (CCA). Reads from higher-depth libraries were subsampled until their total reads per cell were equal. After correcting the batch effect, the data were integrated for z-score normalization. Then, through principal component analysis (PCA), the dimension is reduced. Finally, data clustering was performed using the Seurat R package. The cell types for analysis were derived from the PanglaoDB. Clusters without transcriptional differences were merged into one cluster to avoid overclustering. We used t-distribution random neighborhood embedding (t-SNE) for two-dimensional data visualization. We identified clusters command with the resolution parameter set to 0.5.

Differential Gene Expression Across Control and Psoriasis Mice Groups

A hurdle model in Model-based Analysis of Single-cell Transcriptomics (MAST) was used to find differentially expressed genes for a group in one cluster. We identified differentially expressed genes as following criteria: $|log2FC| \geq 0.36$, p_value_adj ≤ 0.05 and the percentage of cells where the gene was detected in specific cluster is more than 25%. Indigenous differential genes would be used for KEGG enrichment, which was used to discover certain biological functions in each cell type.

Developmental Trajectory Inference

Monocle reduced the space down to one with two dimensions. The cells were ordered (sigma = 0.001, lambda = NULL, param. gamma = 10, tol = 0.001). We identified the key genes may correlate with the development and differentiation process with FDR < 1e-5. Genes that expressed similar reasoning trends were grouped and such groups may share similar biological functions and regulators.

Statistical Analysis

Data analysis was performed using the OmicShare 3 and statistical analyses were performed using GraphPad Prism 8. Unless indicated otherwise stated, the data was expressed as the mean ± SEM. Statistically significant differences used unpaired Student's *t*-test. A value of $P < 0.05$ was considered significant at the 95% confidence level.

Results

Single-Cell RNA-Seq Identified Psoriasis-Associated Immune Cell Populations in Psoriatic Mice

IMQ-induced psoriasis caused by local treatment of 5% IMQ on mouse right ear and back skin was examined. We measured the thickness of the right ear and found that IMQ treatment in the mice resulted in more severe ear swelling than that in control mice (Figure S1A). IMQ treatment induced the symptoms of erythema, scaling and thickening (Figure S1B). H&E staining of the back skin showed epidermal hyperplasia (acanthosis), hyperkeratosis, parakeratosis, micro-abscess and dermal cell infiltration (Figure S1C).

In the scRNA-seq of CD45^{+}-sorted skin cells derived from the back skin of psoriasis mice and C57BL/6 control mice, with stringent filtering at cell and gene levels to eliminate potential doublets, a total of 14,439 cells (2550 WT; 11,889 WT+IMQ) and 17,972 genes were finally captured.

We used t-SNE visualization of the cells to reveal 10 major clusters, including macrophages, NK/T cells, neutrophils, adipocytes, fibroblasts, myocytes, cDCs, endothelial cells, keratinocytes and pDCs (Figure 1A). Each cluster was further
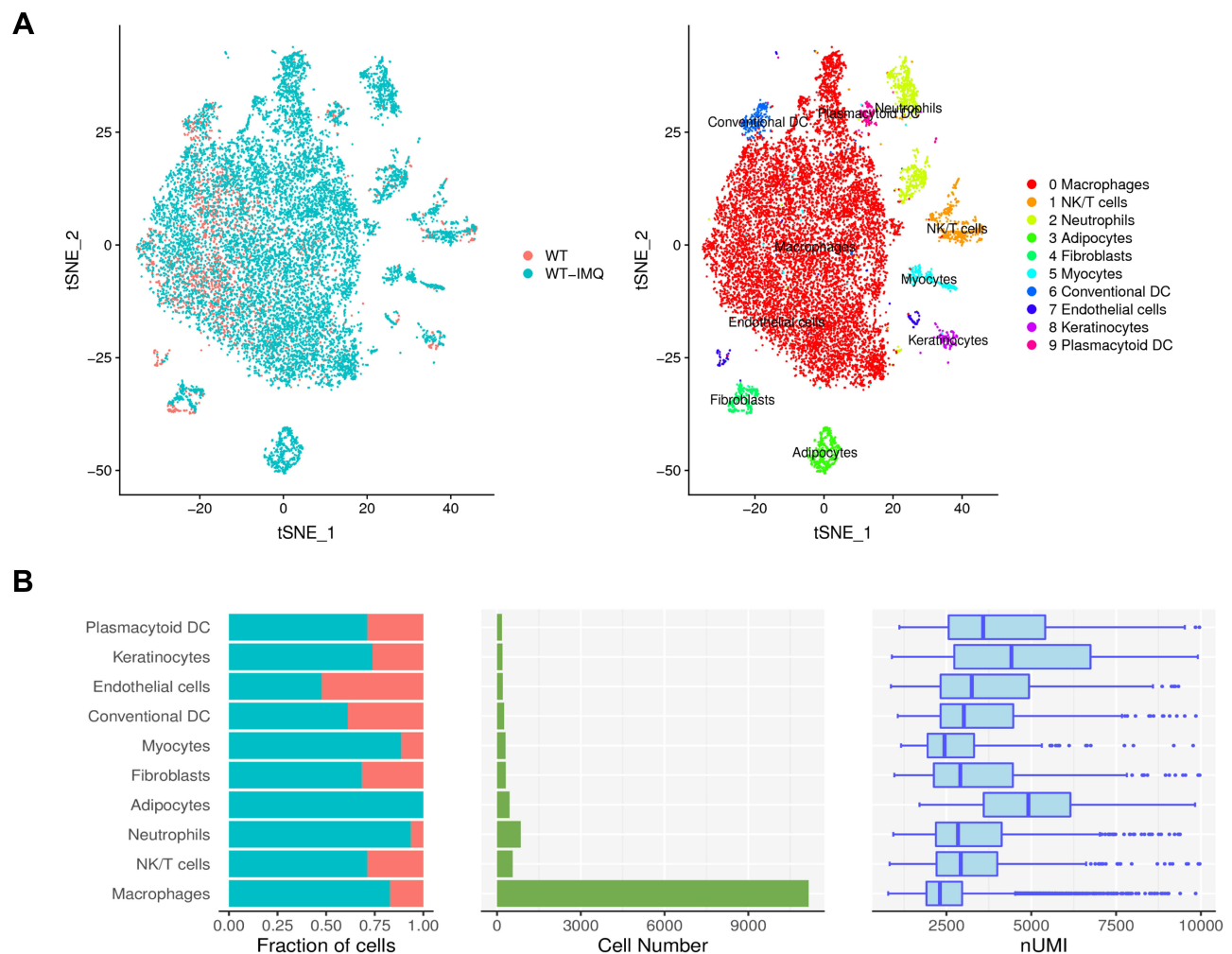
Figure 1 Immune cell populations of back skin biopsies from control and psoriatic mice. (**A**) t-distributed stochastic neighbor embedding (t-SNE) plot depicting 14,439 cells representing 10 immune cell lineages with each cell colour-coded according to sample origin (left panel) and associated cell type (right panel). (**B**) The fraction of cells originating from control (red) and psoriatic mice (blue); the number of cells and box plots of the number of transcripts are shown from left to right.

identified as a specific cell subpopulation according to the expression of the variable genes and the canonical markers, including macrophages (gene markers: *Wfdc17, Adgre1, Pf4*), NK/T cells (*Gzma, Trbc2, Ccl5*), neutrophils (*Retnlg, S100a8, S100a9*), adipocytes (*Adipoq, Plin1, Retn*), and cDCs (*Tnip3, Retnla, Batf3*). In addition, we identified specific genes for most cell populations (Figure S2). All these cell types were widespread in psoriatic samples, indicating the heterogeneous cell composition of skin cells in psoriatic mice.

We observed that the proportions of macrophages, NK/T cells, cDCs and pDCs were increased (Figure 1B), respectively, in accordance with previous observations.[19,20]

Gene Expression Heterogeneity in Macrophage Subsets Was Identified in the Murine Psoriasis

It is known that macrophages play a key role in psoriasis.[21,22] In our study, macrophages increased in psoriatic mice (Figure 1B). Furthermore, we performed IHC analyses of skin biopsies and detected the products of macrophage-associated genes F4/80 enriched in the macrophages. The result showed that F4/80 staining in psoriatic mouse skin lesions was more robust than that in control mice lesions (Figure 2), which was similar to the single-cell RNA-seq.

We grouped all 11,157 macrophages into 7 subgroups using clustering analysis (Figure 3A, S3A), namely, macrophage cluster 0 (*Cd209f*+ *Fcna*+ macrophages), macrophage cluster 1 (*Cd83*+ *Rsad2*+ macrophages), macrophage cluster
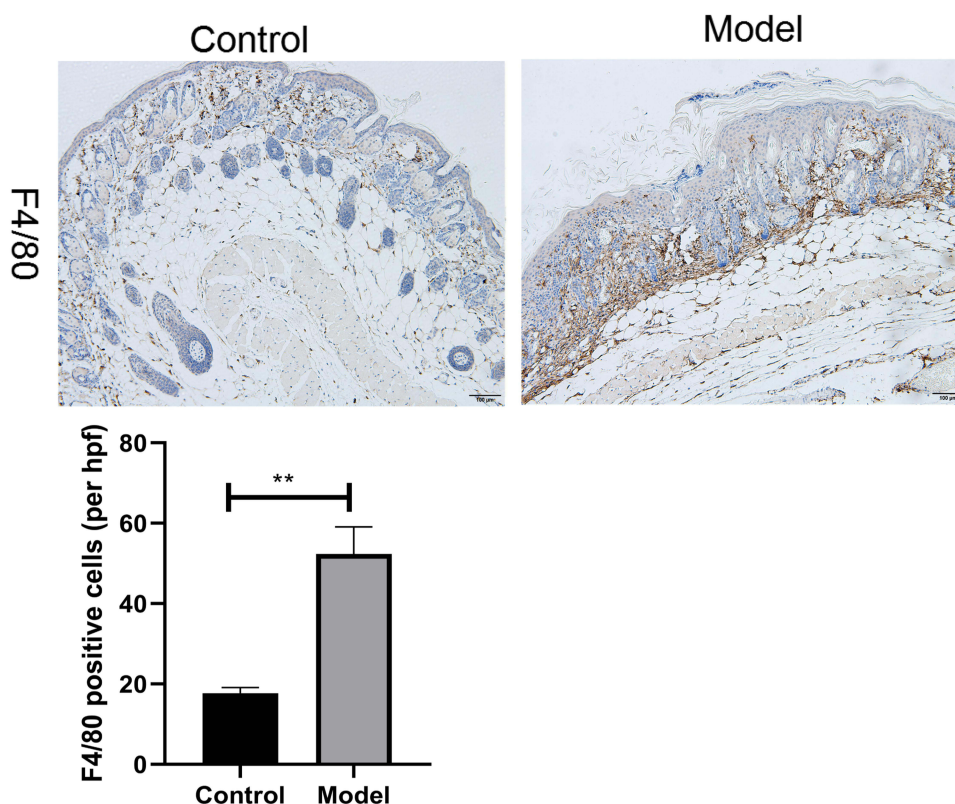
Figure 2 Immunohistochemistry of back skin lesion biopsies from control and psoriatic mice show the expression of F4/80. Quantification of IHC staining from control and psoriatic mouse skin lesions (n = 3) displayed as an average number of positive cells per high-powered field (hpf, × 200), respectively. Scale bar, 100 μm. Data are shown as the mean ± SEM, **P < 0.01.

2 (*Ccl4*^{+} *Bcl2a1b*[+] macrophages), macrophage cluster 3 (*Slamf9*^{+} *Rac2*^{+} macrophages), macrophage cluster 4 (*Vcan*[+] *Thbs1*^{+} macrophages), macrophage cluster 5 (*Ccl8*^{+} *Wfdc17*^{+} macrophages) and macrophage cluster 6 (*Ace*[+] *Treml4*^{+} macrophages). We found that all macrophage clusters increased in psoriatic mice (Figure 3B). *F13a1* and *Lyz2* expressed high levels in all of the macrophage clusters. *Cd209f* was expressed at high level in cluster 0 and *Ccl4* were expressed at high levels in cluster 2. M2-associated gene chitinase-like 3 (*Chil3*) was expressed at high level in cluster 4 and 6. *Saa3* was a unique gene in clusters 0 and 5 (Figure S3B).

To further explore the development of macrophages in psoriasis, we first performed pseudotime trajectory analysis using Monocle2 to order each macrophage cluster along trajectories according to their expression and transition profiles. We identified 9 cell states in macrophages. Next, we observed that macrophages in control mice had the highest pseudotime score meaning the most differentiated and matured macrophages (Figure 3C).

We then performed transcriptome profiling to study the altered genes of macrophages in the psoriatic mice lesions. To identify any gene with a specific expression on a cell type, we performed differential gene expression (DEG) analysis of macrophage clusters. We observed that macrophages in psoriatic mice had widespread overexpression of *Fcgr4, Saa3* and *Acp5* (Figure S4).

Pathway enrichment analysis highlighted that oxidative phosphorylation signaling and antigen processing and presentation signaling were activated in the lesional skin of psoriatic mice. These observations gave us insights into the role of macrophages in psoriatic mice (Figure 3D).

Gene Expression Patterns of NK/T Cells

NK/T cells are significantly increased in psoriatic lesional skin and that are likely implicated in psoriasis pathogenesis.[23,24] We identified a total of 557 NK/T cells based on their transcription of canonical markers (*Gzma, Trbc2, Ccl5*), which were grouped into three cell clusters (Figure 4A, S5A), including NK/T cluster 0 (*Lyz2*^{+} *Ccl6*^{+}), NK/T cluster 1 (*Nkg7*^{+} *Tmsb10*^{+}) and NK/T
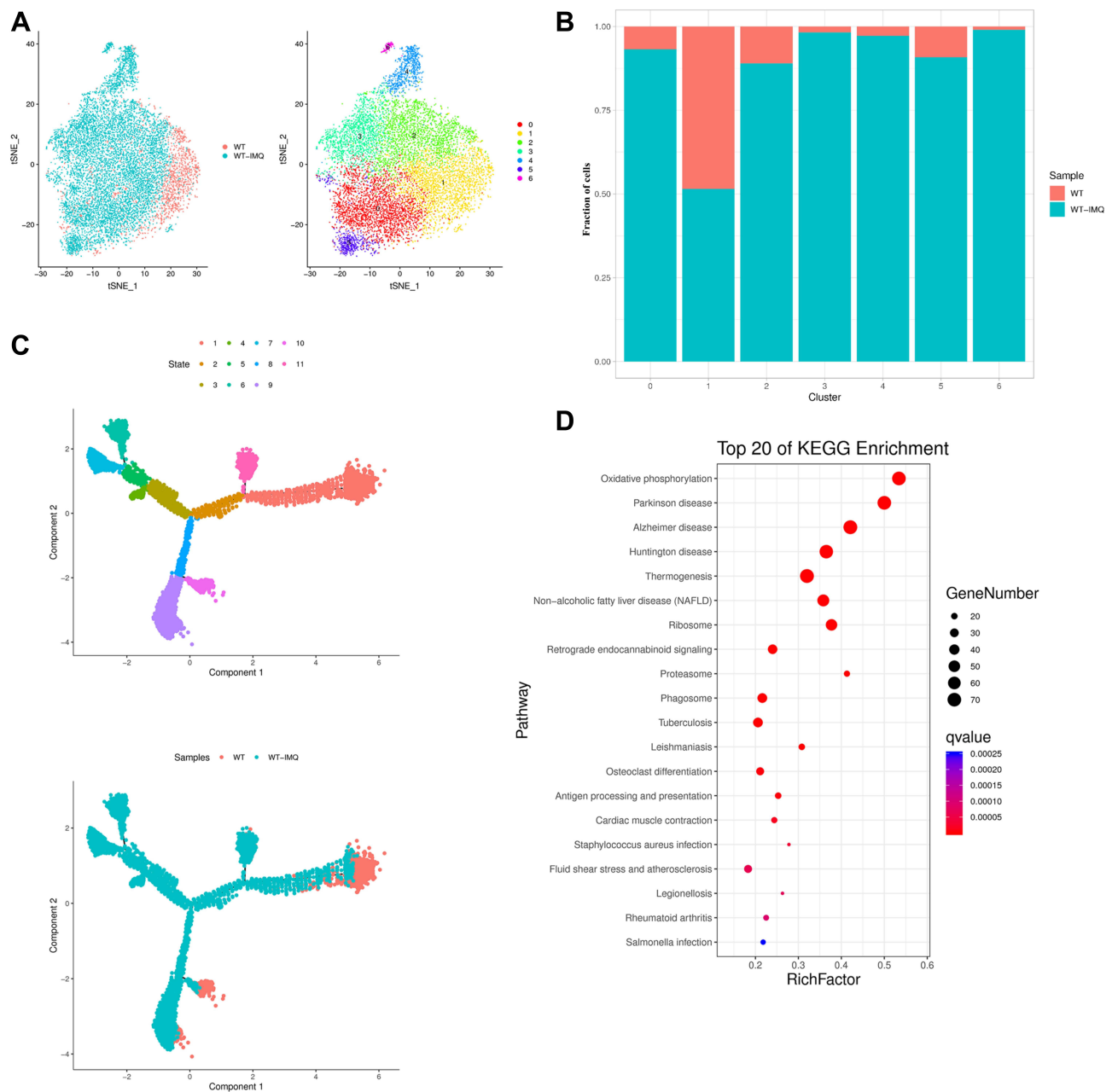
Figure 3 Schematic view of transcriptional characteristics from macrophages. (**A**) t-distributed stochastic neighbor embedding (t-SNE) distributions of the 7 macrophages clusters. (**B**) Bar plots showing cell subset distributions across samples within different groups. Blocks represent individual samples. (**C**) Macrophages trajectory states defined by single cell transcriptomes (top panel) and pseudotime trajectory of macrophages shown separately for control and psoriatic mice (bottom panel). (**D**) Kyoto Encyclopedia of Genes and Genomes (KEGG) analysis of upregulated pathways in macrophages of control mice versus psoriatic mice.

cluster 2 (*Il17f*^{+} *Il17a*^{+}). All NK/T clusters were increased in psoriatic mice. Specifically, the proportion of NK/T cluster 0 (*Lyz2*^{+} *Ccl6*^{+}) in skin biopsies of psoriatic mice increased more significantly (Figure 4B).

Ccl6 and *Lyz2* expressed high levels in three NK/T clusters especially in cluster 0. *Ms4a4b* and *Nkg7* were expressed at high level in cluster 1. *Il17a, Il17f, Il22* and *Tcrg-V6* were unique genes in cluster 2, which was defined as γδ T cells (Figure S5B). It is known that dermal γδT cells are the major IL-17 producers in the skin and may represent a novel target for the treatment of psoriasis.[25–27]

Next, we performed pseudotime trajectory analysis and observed that NK/T cells bifurcated into three branches. NK/T cells cluster 0 was located on the late time of the trajectory. NK/T cells cluster 1 and 2 were located on the early time of
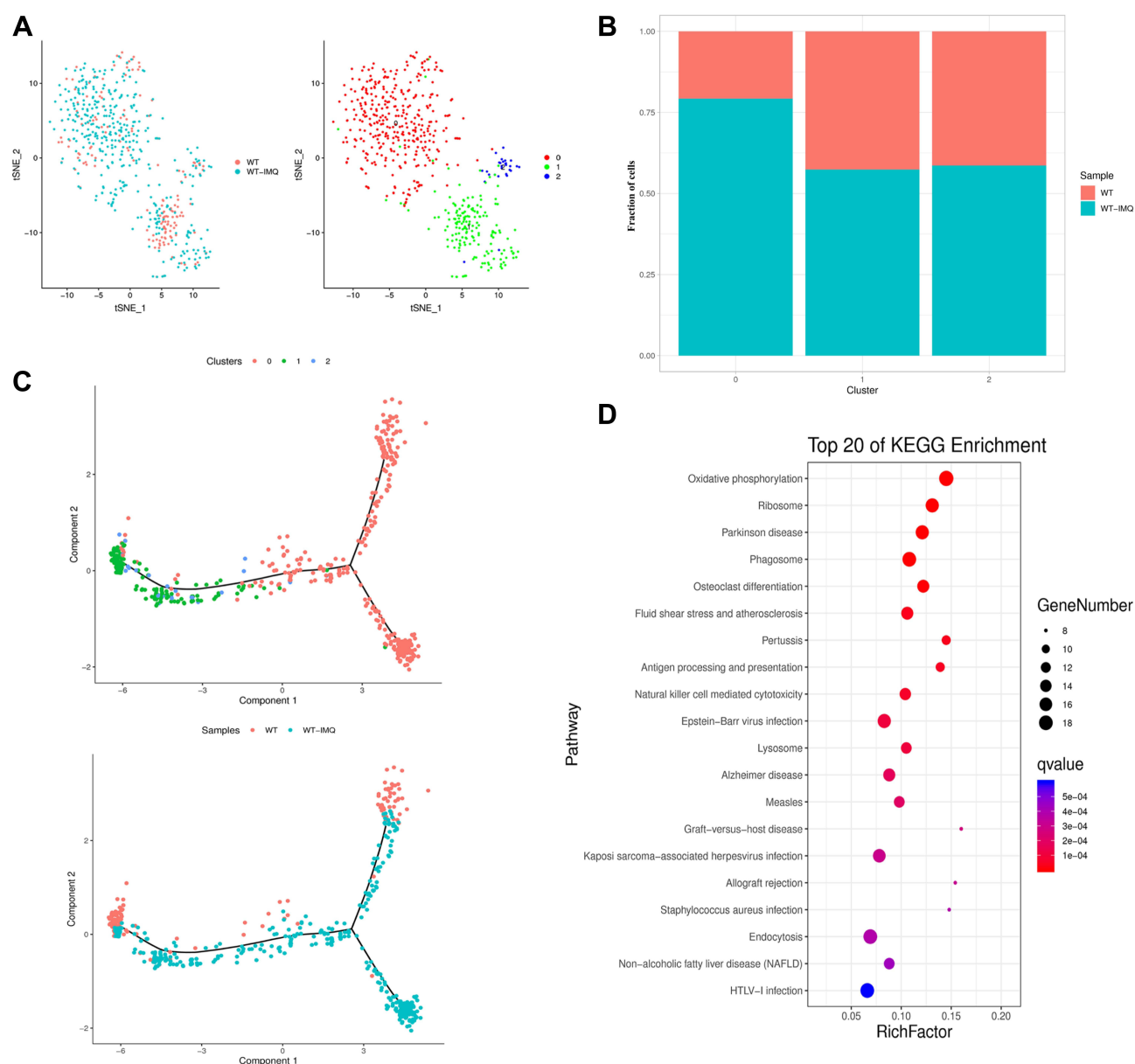
Figure 4 Gene expression heterogeneity in NK/T cells. (**A**) t-distributed stochastic neighbor embedding (t-SNE) distributions of the 3 NK/T cell clusters. (**B**) Bar plots showing cell subset distributions across samples within different groups. Blocks represent individual samples. (**C**) NK/T cells trajectory states defined by single cell transcriptomes (top panel) and pseudotime trajectory of NK/T cells shown separately for control and psoriatic mice (bottom panel). (**D**) Kyoto Encyclopedia of Genes and Genomes (KEGG) analysis of upregulated pathways in NK/T cells of control mice versus psoriatic mice.

the trajectory. NK/T cells in control mice were located on the minor bifurcation of the top right corner and top left corner. NK/T cells in psoriatic mice were located on the right half of the major trajectory (Figure 4C).

Cell-type-specific gene expression differences were also detected in control and psoriatic mice (Figure S4). Heatmap for the expression of *Fcgr4* and *Ms4a6d* demonstrates that these genes were upregulated in NK/T cells from psoriatic mice skin lesions compared to the levels detected in control mice skin lesions. *Ms4a6d* is a member of the MS4A family proteins. Previous results presented that specific MS4A proteins might play distinct roles in infiltrating macrophages and microglia during neuroinflammation.[28]

Signaling pathway enrichment analyses using KEGG revealed a specific pattern of enriched pathways, where the antigen processing and presentation, natural killer cell mediated cytotoxicity and oxidative phosphorylation were significantly upregulated in NK/T cells (Figure 4D).

We further characterized the clonality of NK/T cells using T cell receptor (TCR) repertoire information based on the sequences of α and β chains of TCR, which revealed NK/T cells in psoriatic mice had more clonal NK/T cells, suggesting the clonal expansion of certain dominant clones of NK/T cells (Figure S5C).

Single-Cell Transcriptome Profiling of Conventional Dendritic Cells

We detected a total of 255 cDCs that formed 3 clusters (Figure 5A, S6A). The results showed that cDC cluster 0 was characterized by *Tppp3* and *Med10* expression, cDC cluster 1 was characterized by *Ifnb1* and *Tnfsf9* expression, and cDC
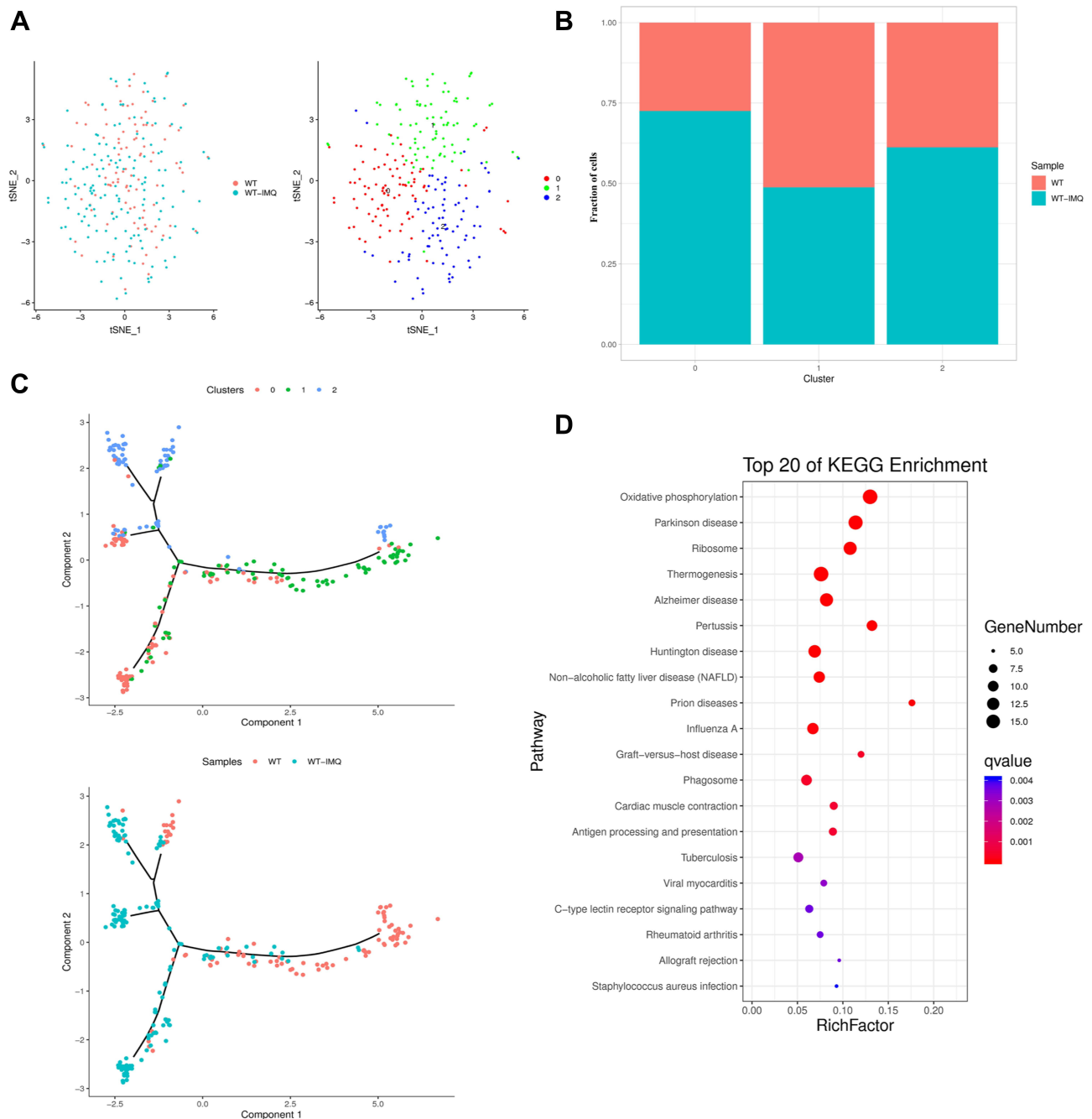
Figure 5 Transcriptome profiling of cDCs in control and psoriatic mice. (**A**) t-distributed stochastic neighbor embedding (t-SNE) distributions of the 3 conventional dendritic cell (cDC) clusters. (**B**) Bar plots showing cell subset distributions across samples within different groups. Blocks represent individual samples. (**C**) cDCs trajectory states defined by single cell transcriptomes (top panel) and pseudotime trajectory of cDCs shown separately for control and psoriatic mice (bottom panel). (**D**) Kyoto Encyclopedia of Genes and Genomes (KEGG) analysis of upregulated pathways in cDCs of control mice versus psoriatic mice.

cluster 2 was characterized by *Gas6* and *Lyve1* expression. Interestingly, we found that cDC clusters 0 and 2 were increased in psoriatic mice while cDC cluster 1 in psoriasis mice was lower than that in the control group (Figure 5B).

S100a6 and *S100a10* involved in inflammation[29] were at high levels in three cDC clusters. *Il1b* and *Il6* expressed high levels in cDC cluster 1. *Clec10a* and *Lyve* were marker genes of cluster 2 (Figure S6B).

To better understand the landscape of cDCs in psoriatic mice versus control mice, we used single-cell trajectory analysis, a machine learning method to embed cells into a linear/branched representation of their gene expression profiles. The results showed that cDC cluster 0 was placed on the bottom left corner, cDC cluster 1 was mainly located on the right half of the trajectory. Pseudotime ordering analysis revealed that cDCs in control mice were located on right half, while the left half of trajectory was occupied by cDCs in psoriatic mice (Figure 5C).

We identified differentially expressed genes in control versus psoriatic mice skin lesions. We focused on the two-fold upregulated or two-fold downregulated genes in psoriatic mice cDCs compared to the levels in control mice. Gene Saa3 was upregulated in cDCs from psoriatic mice skin lesions (Figure S4).

Signaling pathway enrichment analyses using KEGG revealed that oxidative phosphorylation, antigen processing and presentation and graft-versus-host disease were significantly upregulated in cDCs (Figure 5D).

Transcriptomic Profiling of Plasmacytoid Dendritic Cells

We identified 174 pDCs that were assembled into 3 clusters (Figure 6A, S7A). The percentage of pDC cluster 0 (*Cd300a*$^+$ *Ptgs2*$^+$ pDCs), pDC cluster 1 (*Fam213b*$^+$ *Cp*$^+$ pDCs) and 2 (*Ifi205*$^+$ *Cadm1*$^+$ pDCs) were increased in psoriatic mice (Figure 6B, S7A).

Cd209a and *Cd300a* were the marker genes of cluster 0. *F13a1* and *Maf* were unique genes in cluster 1. Cluster 2 was characterized by *Sept3*. We found high expression of *Cst3* in all pDC clusters (Figure S7B).

We observed that pDCs in psoriatic mice had widespread overexpression of *Ifitm1* (Figure S4). Interferon-Induced Transmembrane Protein 1 (IFITM1) was also overexpressed in atopic dermatitis skin lesions,[30] inflamed mucosa of ulcerative colitis[31] and Crohn's disease patients.[32]

We revealed the pDCs lineage differentiation trajectories at single-cell resolution. pDC clusters 0 and 2 were ordered on the left of trajectory, while pDC cluster 1 was ordered on the right of trajectory (Figure 6C).

Pathway enrichment analysis highlighted that TNF signaling pathway, RIG-I-like receptor signaling pathway, toll-like receptor signaling pathway and IL-17 signaling pathway were activated in the lesional skin of psoriatic mice (Figure 6D), which was consistent with the results of previous studies.[33–35]

Discussion

Psoriasis is a prevalent, chronic inflammatory disease of the skin, mediated by immune cells. In our study, C57BL/6 mice were treated with IMQ for 5 consecutive days to induce psoriasis-like dermatitis. Since immune cells are crucial to the progress of psoriasis, we focused on CD45$^+$ cells. Through the comprehensive single-cell transcriptome study on CD45$^+$-sorted skin cells, we provided a landscape view of the heterogeneous cell composition and gene expression heterogeneity in the psoriatic mice at single-cell resolution. Transcriptome analyses of more than 14,439 (2550 WT; 11,889 WT+IMQ) individual cells of 10 cell types revealed two distinct microenvironments between control and psoriatic mice. With such large-scale single-cell data, we identified novel cell populations with specific gene signatures in CD45$^+$-sorted skin cells.

Our scRNA-seq findings indicated that almost all CD45$^+$ cell types (eg, macrophages, NK/T cells, cDCs and pDCs) observed in psoriatic mice were increased, which was basically consistent with the results of human psoriasis sequencing.[16,17] However, B cells and Mast cells that were observed in human psoriasis skin were not observed in our study. Previous research has shown that application of IMQ on mouse skin leads to rapid influx of pDCs.[36] Here, we demonstrate that pDCs increased in psoriatic mice. Similar to our results, DCs also play an important role in human psoriasis single cell sequencing results. Although, here, we divided DCs into cDCs and pDCs for analysis, while in the human psoriasis sequencing data, DCs were divided into mature and semimature DCs for analysis.[15] Here, we found that macrophages were the main group of immune cells in IMQ-induced psoriasis mice, which may explain the reason that regulating macrophages can alleviate IMQ-induced psoriasis symptoms.[37] The number of macrophages was found to increase in the dermis of human psoriasis lesions,[38] but it is worth noting that the scRNA-seq results showed that
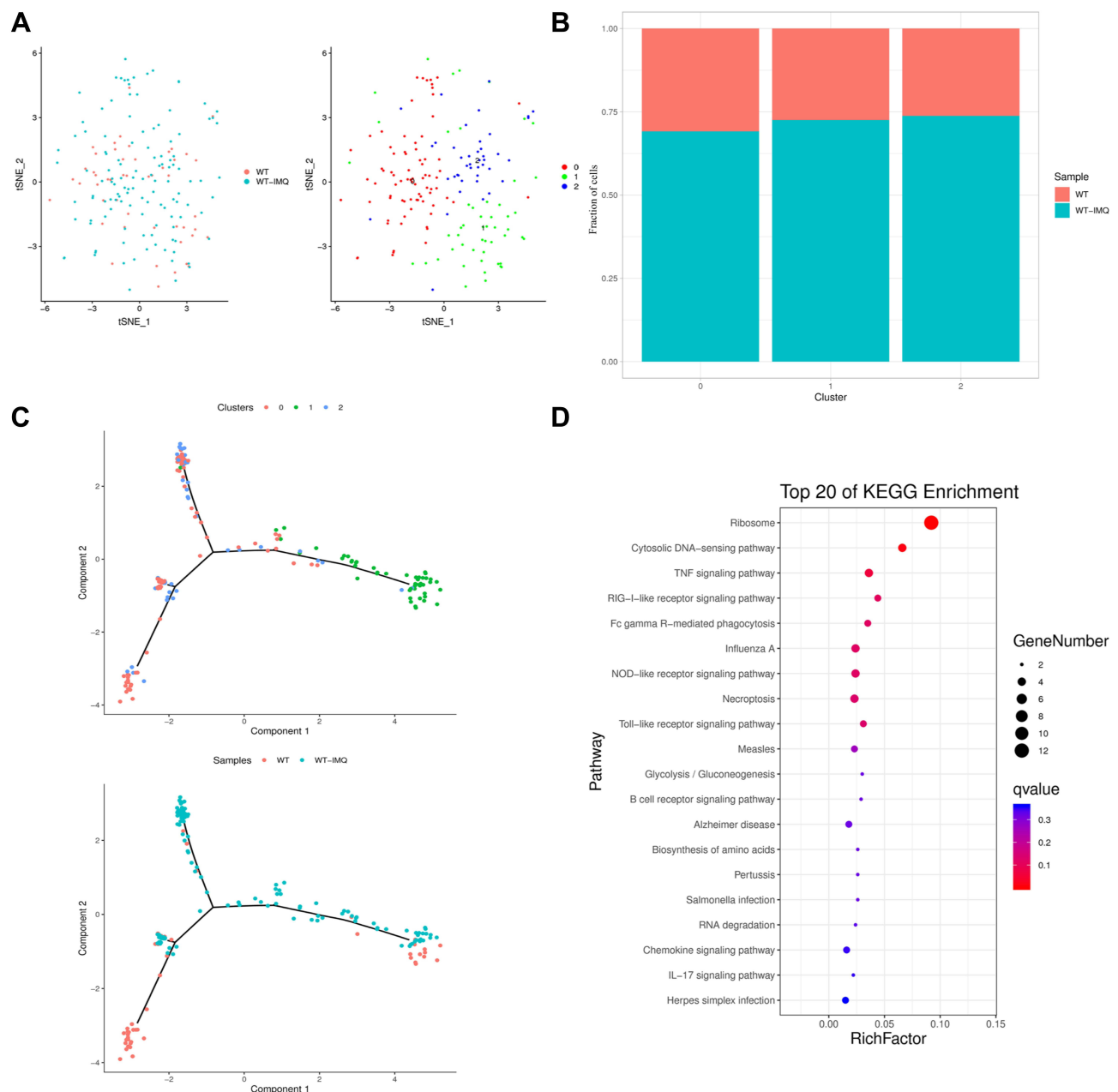
Figure 6 The identification of pDCs in control and psoriatic mice. (**A**) t-distributed stochastic neighbor embedding (t-SNE) distributions of the 3 plasmacytoid dendritic cell (pDC) clusters. (**B**) Bar plots showing cell subset distributions across samples within different groups. Blocks represent individual samples. (**C**) pDCs cells trajectory states defined by single cell transcriptomes (top panel) and pseudotime trajectory of pDCs shown separately for control and psoriatic mice (bottom panel). (**D**) Kyoto Encyclopedia of Genes and Genomes (KEGG) analysis of upregulated pathways in pDCs of control mice versus psoriatic mice.

macrophages accounted for a small proportion in human psoriasis skin.[15] DEG analysis showed that *Fcgr4* and *Saa3* involved in inflammatory response were widely expressed in macrophages of psoriasis mice. *Saa3* contributes to chronic systemic inflammation and has distinct systemic functions in promoting Th17-mediated inflammatory diseases.[39,40] *Fcgr4* (also known as *FcγRIV*) mediates bone erosion in AIA by inducing the influx of S100A8/A9-producing neutrophils into the arthritic joint.[41] *Acp5* encodes tartrate-resistant acid phosphatase (TRAP). Previous research indicated that impaired TRAP functioning may increase susceptibility to sporadic lupus.[42] However, the role of *Saa3* and *Fcgr4* in psoriasis has not been studied, and they may be potential targets for immunotherapy of psoriasis.

As macrophages, NK/T cells, cDCs and pDCs are the main cells involved in the inflammatory network of psoriasis,[43] we further analyzed these four types of cells.

To better understand the transcriptional landscape of immune cells in psoriatic mice versus control mice, we further performed differentiation trajectories in macrophages, NK/T cells, cDCs and pDCs. Macrophages in control mice had the highest pseudotime score meaning the most differentiated and matured macrophages.

Then, we further confirmed differentially expressed genes of different cell types in control versus psoriatic mice skin lesions. Analyses of differentially expressed genes using KEGG revealed the possible mechanisms in different cell types. In pDCs, TNF signaling pathway, RIG-I-like receptor signaling pathway, toll-like receptor signaling pathway and IL-17 signaling pathway were activated in the lesional skin of psoriatic mice. The IL-23/IL-17-mediated inflammatory axis plays a critical role in many inflammatory disorders.[27,44–49] Early studies on the pathogenesis of chronic inflammatory diseases, including rheumatoid arthritis, psoriasis, and inflammatory bowel disease, led to identification of TNF-α as a key trigger of innate inflammatory pathways.[34] Toll-like receptors and RIG-I-like receptor were part of pattern-recognition receptors (PRRs), which are essential for eliciting antiviral immune responses.[50] Moreover, studies have shown that RIG-I is essential for the full development of skin inflammation in IMQ-induced psoriasis-like mouse model.[35] The role of these pathways in IMQ-induced murine psoriasis-like model needs to be focused. In addition, it is interesting that the oxidative phosphorylation signaling pathway was significantly activated in macrophages, NK/T cells and cDCs. Immune cells are closely related to various metabolic processes, including oxidative phosphorylation.[51] It has been reported that Th17 effector cells rely on oxidative phosphorylation to produce energy and cytokines, and inhibiting oxidative phosphorylation can reduce the severity of colitis and psoriasis in mice.[52] In addition, the excessive proliferation of keratinocytes in psoriasis requires oxidative phosphorylation.[53] Therefore, oxidative phosphorylation signaling pathway is closely related to psoriasis, which is worth exploring.

Our research has the following limitations: (1) The immune environment of psoriasis is a dynamic process, but the immune cell profiling detected by our scRNA-seq was a transient state during acute psoriasis inflammation (one day after five consecutive days of IMQ application). (2) Both keratinocytes and immune cells play an important role in the pathogenesis of psoriasis.[54] However, in our study, we focused on CD45+ cells, so the role of keratinocytes was not evaluated; (3) During CD45+ sorting, a small number of immune cells may not be successfully enriched and lost; (4) The specific relationships between enriched pathways in KEGG analysis and psoriasis has not been further studied.

In summary, here, for the first time, we provided a unique insight on the cell-type orchestra in both healthy and psoriatic mice, and uncovered the evolutional conserved/specific skin cell types. Above all, we established the gene expression signatures to better compare IMQ-induced psoriasis model with wild-type mice and clinical psoriasis, and may provide potential therapeutic targets for psoriasis treatment and drug development.

Abbreviations

cDC, conventional dendritic cell; pDC, plasmacytoid dendritic cell; KEGG, Kyoto Encyclopedia of Genes and Genomes; IMQ, Imiquimod; scRNA-seq, single cell RNA sequencing; H&E staining, hematoxylin eosin staining; IHC, immunohistochemistry; GEM, gel bead-in emulsion; UMI, unique molecular index; CCA, canonical correspondence analysis; PCA, principal component analysis; t-SNE, t-distribution random neighborhood embedding; MAST, model-based analysis of single-cell transcriptomic; Chil3, chitinase-like 3; DEG analysis, differential gene expression analysis; TRAP, tartrate-resistant acid phosphatase; TCR, T cell receptor; IFITM1, interferon-induced transmembrane protein 1; PRR, pattern-recognition receptors.

Acknowledgments

Author Contributions

All authors made a significant contribution to the work reported, whether that is in the conception, study design, execution, acquisition of data, analysis and interpretation, or in all these areas; took part in drafting, revising or critically reviewing the article; gave final approval of the version to be published; have agreed on the journal to which the article has been submitted; and agree to be accountable for all aspects of the work.

Funding

Disclosure

The authors report no conflicts of interest in this work.

References

1. Sewerin P, Brinks R, Schneider M, Haase I, Vordenbäumen S. Prevalence and incidence of psoriasis and psoriatic arthritis. *Ann Rheum Dis*. 2019;78(2):286–287. doi:10.1136/annrheumdis-2018-214065
2. Lim DS, Bewley A, Oon HH. Psychological profile of patients with psoriasis. *Ann Acad Med Singap*. 2018;47(12):516–522.
3. López-Ferrer A, Laiz A, Puig L. Psoriatic arthritis. *Med Clin*. 2022;159(1):40–46. doi:10.1016/j.medcli.2022.01.024
4. Yeung H, Takeshita J, Mehta NN, et al. Psoriasis severity and the prevalence of major medical comorbidity: a population-based study. *JAMA Dermatol*. 2013;149(10):1173–1179. doi:10.1001/jamadermatol.2013.5015
5. Damiani G, Pacifico A, Rizzi M, et al. Patients with psoriatic arthritis have higher levels of FeNO than those with only psoriasis, which may reflect a higher prevalence of a subclinical respiratory involvement. *Clin Rheumatol*. 2020;39(10):2981–2988. doi:10.1007/s10067-020-05050-2
6. Conic RR, Damiani G, Schrom KP, et al. Psoriasis and psoriatic arthritis cardiovascular disease endotypes identified by red blood cell distribution width and mean platelet volume. *J Clin Med*. 2020;9(1):186. doi:10.3390/jcm9010186
7. Grän F, Kerstan A, Serfling E, Goebeler M, Muhammad K. Current developments in the immunology of psoriasis. *Yale J Biol Med*. 2020;93(1):97–110.
8. Georgescu SR, Tampa M, Caruntu C, et al. Advances in understanding the immunological pathways in psoriasis. *Int J Mol Sci*. 2019;20(3):739–755. doi:10.3390/ijms20030739
9. Nestle FO, Conrad C, Tun-Kyi A, et al. Plasmacytoid predendritic cells initiate psoriasis through interferon-alpha production. *J Exp Med*. 2005;202(1):135–143. doi:10.1084/jem.20050500
10. Kamata M, Tada Y. Dendritic cells and macrophages in the pathogenesis of psoriasis. *Front Immunol*. 2022;13:941071. doi:10.3389/fimmu.2022.941071
11. Hawkes JE, Chan TC, Krueger JG. Psoriasis pathogenesis and the development of novel targeted immune therapies. *J Allergy Clin Immunol*. 2017;140(3):645–653. doi:10.1016/j.jaci.2017.07.004
12. Chiang CC, Cheng WJ, Korinek M, Lin CY, Hwang TL. Neutrophils in psoriasis. *Front Immunol*. 2019;10:2376. doi:10.3389/fimmu.2019.02376
13. van der Fits L, Mourits S, Voerman JS, et al. Imiquimod-induced psoriasis-like skin inflammation in mice is mediated via the IL-23/IL-17 axis. *J Immunol*. 2009;182(9):5836–5845. doi:10.4049/jimmunol.0802999
14. Flutter B, Nestle FO. TLRs to cytokines: mechanistic insights from the imiquimod mouse model of psoriasis. *Eur J Immunol*. 2013;43(12):3138–3146. doi:10.1002/eji.201343801
15. Kim J, Lee J, Kim HJ, et al. Single-cell transcriptomics applied to emigrating cells from psoriasis elucidate pathogenic vs. regulatory immune cell subsets. *J Allergy Clin Immunol*. 2021;148(5):1281–1292. doi:10.1016/j.jaci.2021.04.021
16. Gao Y, Yao X, Zhai Y, et al. Single cell transcriptional zonation of human psoriasis skin identifies an alternative immunoregulatory axis conducted by skin resident cells. *Cell Death Dis*. 2021;12(5):450. doi:10.1038/s41419-021-03724-6
17. Liu YL, Wang H, Taylor M, et al. Classification of human chronic inflammatory skin disease based on single-cell immune profiling. *Sci Immunol*. 2022;7(70):eabl9165. doi:10.1126/sciimmunol.abl9165
18. Paik DT, Cho S, Tian L, Chang HY, Wu JC. Single-cell RNA sequencing in cardiovascular development, disease and medicine. *Nat Rev Cardiol*. 2020;17(8):457–473. doi:10.1038/s41569-020-0359-y
19. Lowes MA, Suárez-Fariñas M, Krueger JG. Immunology of psoriasis. *Annu Rev Immunol*. 2014;32:227–255. doi:10.1146/annurev-immunol-032713-120225
20. Lowes MA, Bowcock AM, Krueger JG. Pathogenesis and therapy of psoriasis. *Nature*. 2007;445(7130):866–873. doi:10.1038/nature05663
21. Nestle FO, Di Meglio P, Qin JZ, Nickoloff BJ. Skin immune sentinels in health and disease. *Nat Rev Immunol*. 2009;9(10):679–691. doi:10.1038/nri2622
22. Qie C, Jiang J, Liu W, et al. Single-cell RNA-Seq reveals the transcriptional landscape and heterogeneity of skin macrophages in Vsir -/- murine psoriasis. *Theranostics*. 2020;10(23):10483–10497. doi:10.7150/thno.45614
23. Gudjonsson JE, Kabashima K, Eyerich K. Mechanisms of skin autoimmunity: cellular and soluble immune components of the skin. *J Allergy Clin Immunol*. 2020;146(1):8–16. doi:10.1016/j.jaci.2020.05.009
24. Liu J, Chang HW, Huang ZM, et al. Single-cell RNA sequencing of psoriatic skin identifies pathogenic Tc17 cell subsets and reveals distinctions between CD8 + T cells in autoimmunity and cancer. *J Allergy Clin Immunol*. 2021;147(6):2370–2380. doi:10.1016/j.jaci.2020.11.028
25. Cai Y, Shen X, Ding C, et al. Pivotal role of dermal IL-17-producing γδ T cells in skin inflammation. *Immunity*. 2011;35(4):596–610. doi:10.1016/j.immuni.2011.08.001
26. Jee MH, Mraz V, Geisler C, Bonefeld CM. γδ T cells and inflammatory skin diseases. *Immunol Rev*. 2020;298(1):61–73. doi:10.1111/imr.12913
27. Bugaut H, Aractingi S. Major role of the IL17/23 axis in psoriasis supports the development of new targeted therapies. *Front Immunol*. 2021;12:621956. doi:10.3389/fimmu.2021.621956
28. DePaula-Silva AB, Gorbea C, Doty DJ, et al. Differential transcriptional profiles identify microglial- and macrophage-specific gene markers expressed during virus-induced neuroinflammation. *J Neuroinflammation*. 2019;16(1):152–171. doi:10.1186/s12974-019-1545-x
29. Eckert RL, Broome AM, Ruse M, Robinson N, Ryan D, Lee K. S100 proteins in the epidermis. *J Invest Dermatol*. 2004;123(1):23–33. doi:10.1111/j.0022-202X.2004.22719.x
30. Rebane A, Zimmermann M, Aab A, et al. Mechanisms of IFN-γ-induced apoptosis of human skin keratinocytes in patients with atopic dermatitis. *J Allergy Clin Immunol*. 2012;129(5):1297–1306. doi:10.1016/j.jaci.2012.02.020

31. Hisamatsu T, Watanabe M, Ogata H, et al. Interferon-inducible gene family 1–8U expression in colitis-associated colon cancer and severely inflamed mucosa in ulcerative colitis. *Cancer Res*. 1999;59(23):5927–5931.

32. Wu F, Dassopoulos T, Cope L, et al. Genome-wide gene expression differences in Crohn's disease and ulcerative colitis from endoscopic pinch biopsies: insights into distinctive pathogenesis. *Inflamm Bowel Dis*. 2007;13(7):807–821. doi:10.1002/ibd.20110

33. Blauvelt A, Chiricozzi A. The immunologic role of IL-17 in psoriasis and psoriatic arthritis pathogenesis. *Clin Rev Allergy Immunol*. 2018;55 (3):379–390. doi:10.1007/s12016-018-8702-3

34. Zaba LC, Suárez-Fariñas M, Fuentes-Duculan J, et al. Effective treatment of psoriasis with etanercept is linked to suppression of IL-17 signaling, not immediate response TNF genes. *J Allergy Clin Immunol*. 2009;124(5):1022–10.e1–395. doi:10.1016/j.jaci.2009.08.046

35. Zhu H, Lou F, Yin Q, et al. RIG-I antiviral signaling drives interleukin-23 production and psoriasis-like skin disease. *EMBO Mol Med*. 2017;9 (5):589–604. doi:10.15252/emmm.201607027

36. Palamara F, Meindl S, Holcmann M, Lührs P, Stingl G, Sibilia M. Identification and characterization of pDC-like cells in normal mouse skin and melanomas treated with imiquimod. *J Immunol*. 2004;173(5):3051–3061. doi:10.4049/jimmunol.173.5.3051

37. Yang L, Fu JR, Han X, et al. Hsa_circ_0004287 inhibits macrophage-mediated inflammation in an N 6-methyladenosine-dependent manner in atopic dermatitis and psoriasis. *J Allergy Clin Immunol*. 2022;149(6):2021–2033. doi:10.1016/j.jaci.2021.11.024

38. Nakamizo S, Dutertre CA, Khalilnezhad A, et al. Single-cell analysis of human skin identifies CD14+ type 3 dendritic cells co-producing IL1B and IL23A in psoriasis. *J Exp Med*. 2021;218(9):e20202345. doi:10.1084/jem.20202345

39. den Hartigh LJ, Wang S, Goodspeed L, et al. Deletion of serum amyloid A3 improves high fat high sucrose diet-induced adipose tissue inflammation and hyperlipidemia in female mice. *PLoS One*. 2014;9(9):e108564. doi:10.1371/journal.pone.0108564

40. Lee JY, Hall JA, Kroehling L, et al. Serum amyloid A proteins induce pathogenic Th17 cells and promote inflammatory disease. *Cell*. 2020;183 (7):2036–2039. doi:10.1016/j.cell.2020.12.008

41. Di Ceglie I, Ascone G, Cremers NAJ, et al. Fcγ receptor-mediated influx of S100A8/A9-producing neutrophils as inducer of bone erosion during antigen-induced arthritis. *Arthritis Res Ther*. 2018;20(1):80. doi:10.1186/s13075-018-1584-1

42. An J, Briggs TA, Dumax-Vorzet A, et al. Tartrate-resistant acid phosphatase deficiency in the predisposition to systemic lupus erythematosus. *Arthritis Rheumatol*. 2017;69(1):131–142. doi:10.1002/art.39810

43. Vičić M, Kaštelan M, Brajac I, Sotošek V, Massari LP. Massari, current concepts of psoriasis immunopathogenesis. *Int J Mol Sci*. 2021;22 (21):11574. doi:10.3390/ijms222111574

44. Clarke J. IL-17 sustains plasma cells in SLE. *Nat Rev Rheumatol*. 2020;16(12):666. doi:10.1038/s41584-020-00519-5

45. Faust HJ, Zhang H, Han J, et al. IL-17 and immunologically induced senescence regulate response to injury in osteoarthritis. *J Clin Invest*. 2020;130(10):5493–5507. doi:10.1172/JCI134091

46. Regen T, Isaac S, Amorim A, et al. IL-17 controls central nervous system autoimmunity through the intestinal microbiome. *Sci Immunol*. 2021;6 (56):eaaz6563. doi:10.1126/sciimmunol.aaz6563

47. Ghoreschi K, Balato A, Enerbäck C, Sabat R. Therapeutics targeting the IL-23 and IL-17 pathway in psoriasis. *Lancet*. 2021;397(10275):754–766. doi:10.1016/S0140-6736(21)00184-7

48. Lou F, Sun Y, Xu Z, et al. Excessive polyamine generation in keratinocytes promotes self-rna sensing by dendritic cells in psoriasis. *Immunity*. 2020;53(1):204–216.e10. doi:10.1016/j.immuni.2020.06.004

49. Nakajima K. Critical role of the interleukin-23/T-helper 17 cell axis in the pathogenesis of psoriasis. *J Dermatol*. 2012;39(3):219–224. doi:10.1111/j.1346-8138.2011.01458.x

50. Okude H, Ori D, Kawai T. Signaling through nucleic acid sensors and their roles in inflammatory diseases. *Front Immunol*. 2021;11:625833. doi:10.3389/fimmu.2020.625833

51. Piranavan P, Bhamra M, Perl A. Metabolic targets for treatment of autoimmune diseases. *Immunometabolism*. 2020;2(2):e200012. doi:10.20900/immunometab20200012

52. Franchi L, Monteleone I, Hao LY, et al. Inhibiting oxidative phosphorylation in vivo restrains Th17 effector responses and ameliorates murine colitis. *J Immunol*. 2017;198(7):2735–2746. doi:10.4049/jimmunol.1600810

53. Liszewska A, Robak E, Bernacka M, Bogaczewicz J, Woźniacka A. Methotrexate use and NAD+/NADH metabolism in psoriatic keratinocytes. *Postepy Dermatol Alergol*. 2020;37(1):19–22. doi:10.5114/ada.2020.93379

54. Ortonne JP. Aetiology and pathogenesis of psoriasis. *Br J Dermatol*. 1996;135(Suppl 49):1–5. doi:10.1111/j.1365-2133.1996.tb15660.x